



Internal Report submitted to the USC Office of Research, USC Department of Physics and Space Environment Research Center (SERC), Kyushu University:

# Space Weather, Seismo-Electromagnetics and the MAGnetic Data Acquisition System (MAGDAS)-Philippine Sector

---

R. E. S. Otadoy and R. Violanda

Department of Physics, University of San Carlos, Cebu City, Philippines

A. Albano

Bryn Mawr College, Bryn Mawr, Pennsylvania, USA

D. McNamara

The Manila Observatory, Ateneo de Manila University, Quezon City, Philippines

MAGDAS Group

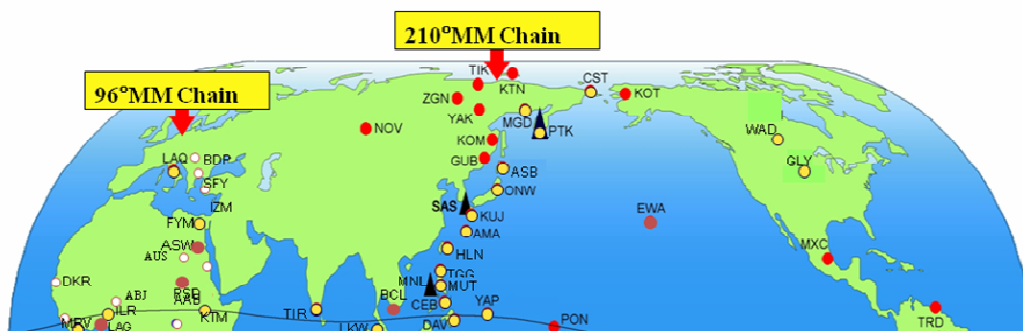
Space Environment Research Center, Kyushu University, Fukuoka, Japan

## Executive Summary

This document is an internal report of the USC Department of Physics' involvement in the MAGDAS project, which is the reason why the Geophysics Group was established. Throughout the years of this collaboration, we have identified studies in equatorial electrojet and seismo-electromagnetics as our research focus because of their importance to the Philippine situation. We have selected two recent publications of the MAGDAS Group as jumping board for our research. The first one is about an algorithm to construct a new index, called EE-Index (equatorial electrojet index) used for studies in equatorial electrojet and counter electrojet (Uozumi et al., 2008). This new index consists of  $EDst$ , which closely follows the variation of the well known  $Dst$  index,  $EU_s(m)$ , and  $EL_s(m)$ . The latter two quantities are obtained by subtracting  $EDst$  from the original northward magnetic data. It turns out that  $EU_s(m)$  is appropriate for the investigation of EEJ and  $EL_s(m)$  for CEJ. The other paper is about a new wave analysis technique to extract ULF precursory signals from the MAGDAS data (Yumoto et al. 2009). We extend these studies by

using nonlinear and time series analyses introduced by Dr. Alfonso Albano, who is a Balik-Scientist grantee from Bryn Mawr College, Pennsylvania, USA. Dr. Albano will conduct a workshop on these techniques on June 23-30, 2010. It is hoped that this workshop will jumpstart research in this area.

## 1.Introduction



The Geophysics Group of the Department of Physics was established as an outgrowth of our collaboration with the Space Environment Research Center (SERC), Kyushu University in the MAGDAS (MAGnetic Data Acquisition System) project. MAGDAS is a globally dense network of magnetometers installed to monitor the geomagnetic field in real-time from different locations on the surface of the earth. Since variations of the earth's magnetic field are primarily influenced by geospace environmental conditions, magnetic data available from this network allows ground-based monitoring of space weather. Due to the impact of space weather disturbances, such as space storms, to space-based and ground-based installations, space weather monitoring is nowadays becoming an important component of disaster prevention and mitigation. Recently, an enormous amount of data suggests that electromagnetic signals may occur before, during, and after the occurrence of an earthquake and the science that deals with them is called *seismoelectromagnetics*. Signals occurring before an earthquake are called *electromagnetic earthquake precursors* and are used as possible early warning system for an impending earthquake. It turns out that the good geomagnetic data available from MAGDAS are valuable in the search for EM earthquake precursors.

MAGDAS is the successor of the Circum Pan-Pacific Magnetometer Network (CPMN) installed by the Space Environment Research Center (SERC), Kyushu University, during the period (1990-1997) of the Solar-Terrestrial Energy Program (STEP) (Yumoto and the CPMN Group 2001). The network practically covers the polar, mid-latitude, and equatorial regions. The 1-sec and 1-minute magnetic field data generated by this ground-based array of magnetometers allow a coordinated investigation of geospace plasma (ionospheric and magnetospheric) processes by distinguishing between temporal and spatial variations, clarify global structures and propagation characteristics from higher to equatorial latitudes, and understand the global generation mechanisms of the solar-terrestrial phenomena. SERC then collaborated with about 30 international organizations to achieve its goals. Starting 2005, SERC has established a new real-time Magnetic Data Acquisition System in the CPMN (MAGDAS/CPMN) region and an FM-CW radar network along the 210° magnetic meridian for space weather research and other applications (Yumoto and the MAGDAS group, 2007). New fifty fluxgate magnetometers with a spacing of about 500 km were

installed from Davis Station (Australia Antarctic Division station) in the Antarctica all the way to Cape Schmidt in northern Siberia as shown in Figure 1.

The MAGDAS/CPMN magnetometer unit consists of 3-axial ring-core sensors, fluxgate-type magnetometer, data logging/transferring unit, and power supply as shown in Figure 2. Magnetic field digital data are obtained at the sampling rate of 1/16 second. The averaged data are transferred from overseas stations to SERC in near real time using the internet. The ambient magnetic field, expressed by horizontal (H), declination (D), and vertical (Z) components, is digitized by using the field-canceling coils for the dynamic range of  $\pm 64,000$  nT/16bit. Three observation ranges of  $\pm 2,000$  nT,  $\pm 1,000$  nT, and  $\pm 300$  nT for high, middle, and low-latitude stations, respectively, are available. The resolution of MAGDAS data are 0.061 nT/LSB and 0.031 nT/LSB, and 0.0091 nT/LSB for the  $\pm 2,000$ -nT and  $\pm 1,000$ -nT, and  $\pm 300$ -nT ranges, respectively. The estimated noise level of the MAGDAS magnetometers is 0.02 nTp-p. The data logger/transfer unit is provided with a GPS antenna for time adjustment. Data are logged into the Compact Flash Memory Card of 1 GB. The total weight of the compact MAGDAS magnetometer system is less than 15 kg.

To date, MAGDAS/CPMN is the most extensive magnetometer network in the world. This new installation can now be used to monitor the global electromagnetic and plasma environment in geospace in order to gain a better understanding of the complex sun-earth coupling. MAGDAS/CPMN aims to continuously monitor the earth's electromagnetic environment and utilize the observations for forecasting changes in space and lithosphere conditions. This project is actively providing information about the space weather condition through the following: (1) global 3-dimensional current system—to know electromagnetic (EM) coupling of field-aligned currents, auroral electrojet current, Sq current, and equatorial electrojet current; (2) plasma mass density along the 210° MM—to understand the plasma environment change during space storms; (3) 24-hour monitoring of the ionospheric drift velocity by the FM-CW radar with 10-sec sampling at L=1.26 to understand how the external electric field penetrates into the equatorial ionosphere (see Yumoto and the MAGDAS group, 2006). Recently, SERC has installed a magnetometer chain along the 96° magnetic meridian. This magnetometer network, called MAGDAS II, straddles primarily on the African continent as can be seen in Figure 1.

In the Philippines SERC initiated collaborations with different institutions to establish four MAGDAS magnetic observatories. These are found in Tuguegarao, Cagayan (Cagayan State University), Muntinlupa (Coast and Geodetic Survey Department, National Mapping and Resource Information Authority-NAMRIA), Cebu (USC Department of Physics), and Davao (Shrine Hill, which is administered by the Manila Observatory). In 2009, two additional MAGDAS magnetic observatories were established: Legazpi (Divine Word College of Legazpi) and Cagayan de Oro (Xavier University). Shown in Table 1 are the MAGDAS magnetic observatories located in the Philippines with the corresponding geographic latitudes/longitudes, geomagnetic latitudes/longitudes, L-values, and the dip latitudes.

In this report, we outline the scientific contribution of MAGDAS to the Philippines and future prospects for research. First a background on sun-earth interaction will be given to put the reader in the proper perspective. Next, a discussion on two important papers [Yumoto et al. 2009, Uozumi et al. 2008] which we think are important to the Philippine situation will be portrayed. Finally, future research prospects will be delineated.

## **1.1. The Solar Wind and Space Weather: Space Storms**

Physical processes occurring in space have correlations with terrestrial and atmospheric phenomena. This is more apparent in studies on the earth's space environment, which primarily includes the ionosphere and the overlying region, the magnetosphere. The importance of space environment was first recognized when radio waves were first used in wireless communications. Although not known during the pioneering works on long distance radio transmission, the ionosphere-earth system acts as a waveguide for radio waves which make long-distance communication possible. Nowadays, studies in space environment become more urgent because of its impact on terrestrial and space-based installations. Earth's space environment is formed and strongly influenced by the interaction of the sun-earth system. Thus, an understanding of space environment requires investigation of the processes occurring in the sun, earth, and the intervening space.

The temperature of the outermost solar atmosphere, called the *solar corona*, is about a million Kelvin. At this temperature, solar atmospheric gas (mainly hydrogen) is almost completely ionized into negatively charged electrons and positive ions that form a globally neutral gas or fluid of negatively and positively charged particles called *plasma*. Due to the extremely hot condition in the sun's atmosphere, solar plasma cannot be in static equilibrium. Streams of charged particles comprising the plasma flow at supersonic speeds (about 500 km per second) bringing along the sun's electromagnetic fields into interplanetary space. The outflow of the stream of plasma into interplanetary space is called the *solar wind*. Through it, the sun's magnetic field extends into interplanetary space and is called the *interplanetary magnetic field* (IMF). The interaction of the solar wind and the earth's magnetic field shapes the magnetosphere (Lyon 2000). The geomagnetic field is strong enough that the solar wind can approach the earth within a minimum distance of about 10 Earth radii at the dayside (the front side directly facing the sun) effectively confining the geomagnetic field at that distance as shown in Figure 3.

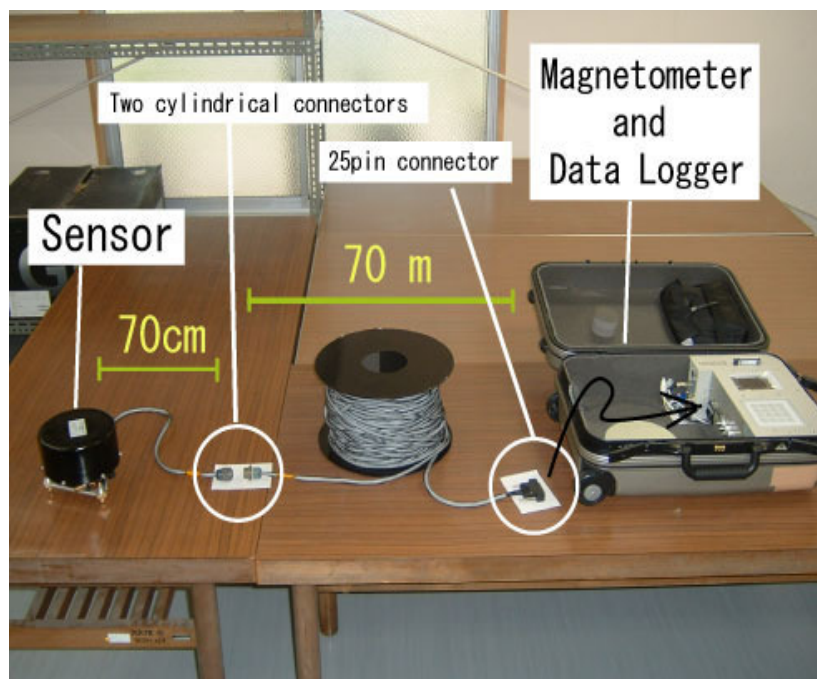


Figure 2. The MAGDAS/CPMN magnetometer components.

The streaming charged particles in the solar wind would be deflected forming the boundary between the magnetosphere and the solar wind, called the *magnetopause*. At the night side, the solar wind veers the geomagnetic field away forming an elongated tail-like structure called the *magnetotail*. Propagating at supersonic speed, the solar wind would form a bow shock when it collides with the earth. The region between the bow shock and the magnetopause is called the *magnetosheath*. Solar wind particles are injected into the magnetosphere, generating current through a magnetohydrodynamic process called the *solar wind-magnetosphere generator or auroral generator* (Akasofu 1968). In this process the kinetic energy of the solar wind particles is converted into electric current generating more than a million of megawatts of electric power. Injection of large amount of energy into the ionosphere by the auroral generator occurs through a pair of electric currents, called *eastward and westward electrojets*. These jet currents produce magnetic field variations on the ground.

Cataclysmic release of energy from the sun, such as due to solar flares and coronal mass ejections, induces abrupt changes in the solar wind that drastically alter the electromagnetic and particle environment of the earth, a phenomenon called *magnetic or space storm*. In analogy with atmospheric phenomena, the term *space weather* is coined to refer to conditions in the earth's space environment. During transient releases of energy from the sun, a shock wave is generated and propagates in the solar wind with velocity range of 500-1000 km/s just behind the wavefront. As the shock wave collides with the Earth's magnetosphere, the power of the solar wind-magnetosphere generator may surge to about 10 million megawatts or higher giving rise to geomagnetic storm. During this space weather phenomenon, large-amplitude and prolonged southward component of the IMF enhances the magnetospheric convection of energetic ions and electrons from the near-earth magnetotail to the inner magnetosphere which forms and intensifies the ring current. The ring current brings about large deviations in the geomagnetic field on the ground.

Table 1. MAGDAS/CPMN magnetic stations in the Philippines (<http://magdas.serc.kyushu-u.ac.jp/station/index.html>).

Abbreviation	Station Name	Geog. Latitude	Geog. Longitude	Geomag. Latitude	Geomag. Longitude	L	Dip Latitude
TUG	Tuguegarao	17.66	121.76	10.26	193.05	1.03	
MUT	Muntinlupa	14.37	121.02	6.79	192.25	1.01	6.79
LGZ	Legazpi	13.15	123.74	5.48	194.92	1.01	5.49
CEB	Cebu	10.36	123.91	2.53	195.06	1.00	2.74
CDO	Cagayan de Oro	8.46	124.63	0.52	195.77	1.00	0.77
DAV	Davao	7.00	125.40	-1.02	196.54	1.00	-0.65

Space storms have been known to pose danger on space-based and terrestrial installations. For instance highly energetic charged particles can damage equipment, such as solar cells, carried by spacecrafts. They also pose health hazards to astronauts working in space and can increase orbital drag of earth-orbiting satellites resulting to their diminished lifetime. They can also disrupt satellite communications. Considering the fact that the ionosphere acts as waveguide in radio propagation over the surface of the earth, disturbance in the ionosphere due to space storms may also disrupt radio communication. Geomagnetic

disturbance also produces potential gradients, thereby inducing geoelectric fields on the earth's crust driving geomagnetically induced currents (GIC). The magnitude of GICs depends on the intensity of the space storm, latitude of the location, and ground resistivity. GICs are higher in the auroral regions where geomagnetic variations are large and rapid. Quasi-dc geomagnetically induced currents were reported to enter neutral points in grounded power transformers and therefore flow through transformer windings and into power transmission lines. This resulted to saturation of transformer cores and instability of the power system which eventually led to power failure. The most prominent case of the impact of GIC on power plants was the breakdown of Hydro-Quebec power system during an intense storm in March 1989 (Boteler et. al. 1989). In more general terms, planet earth is livable because of the protective shield provided by the geomagnetic field from solar wind particles and radiation. However, there are instances that this protective shield is breached, e.g. during intense space storms. Understanding the underlying processes in sun-earth coupling is as crucial as understanding climate change for the survival of mankind. All these dangers posed by geomagnetic storms warrant investments for research in space environment and space weather.

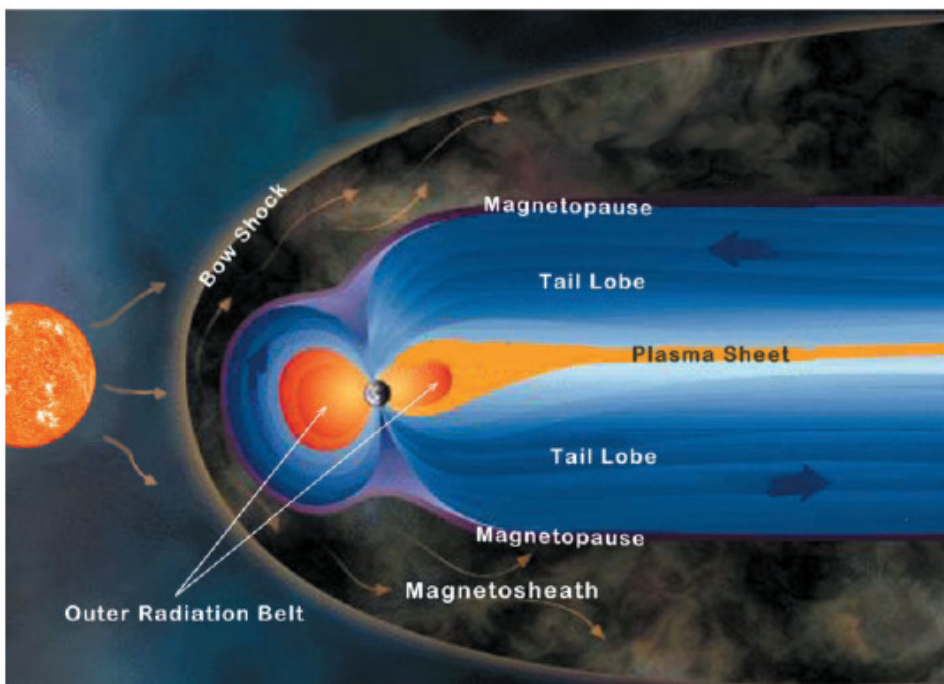


Figure 3. Schematic portrait of the interaction between the solar wind and the geomagnetic field. Adopted from (Lyon 2007).

### 1.3. Seismoelectromagnetics

In recent years, electromagnetic (EM) earthquake precursors in the wide band of frequencies (from ULF to optical) were observed (Gokhberg 1982; Park et al. 1993; Oike and Yamada 1994; Hayakawa et al. 1996; Hayakawa et al. 2000; Hashimoto et al. 2002; Bleier and Freund 2005). In addition, changes in magnetospheric and ionospheric parameters correlated well with the impending occurrence of an

earthquake and strain induced on the ground due to crustal activity also produces changes in ground conductivity (Park et al. 1993). Development of a robust method of detecting these precursors will pave the way for a possible early warning system of impending earthquakes.

## **1.4. Research Thrust**

Due to the Philippine's proximity to the equator, the focus of our involvement in space weather research is on the study of equatorial electrojet (Otadoy et al.). Equatorial electrojet (EEJ) is a band of enhanced ionospheric current in a narrow strip along the dip equator caused by an enhancement of east-west Cowling conductivity (Forbes 1981). By utilizing this network of ground-based instruments, it is hoped that their regular day-to-day and seasonal variabilities and variations during magnetic storms and substorms will be understood.

One can see in Figure 1 that the magnetometer array along the dip equator encompasses the full longitudinal range (*i.e.*, practically around the globe). A study of the equatorial electrojet using the MAGDAS/CPMN thus allows investigation of the global characteristics of this ionospheric current system. It is well known that the equatorial region is the terminal region of energy flows in the earth's space environment. With the MAGDAS/CPMN's north to south ground-based magnetometer network along the 210° magnetic meridian, the equatorial electrojet can be studied as part of a global circuit (Kobea et al. 1998). The additional MAGDAS magnetic observatories in Legazpi and Cagayan de Oro will allow understanding of the spatial structure of EEJ in the Philippines. Since solar-terrestrial disturbances penetrate the equatorial ionosphere, understanding of these disturbances at the dip equator allows nowcasting of these phenomena in the solar wind region.

In addition, since the Philippines is sitting on the Pacific Ring of Fire, it is susceptible to frequent tremors due to volcanic activity or due to movements of the earth's crust. An early warning system for earthquakes can save both lives and property. Geologists have been studying earthquakes for years in the hope of understanding this crustal phenomenon and eventually develop the capability to predict its occurrence. However, decades of research can only give the probability that an earthquake occurs in a particular area in the long term. Short-term earthquake warning system can certainly save lives and property.

Although a new ULF wave analysis to extract earthquake precursors from the MAGDAS data has already been established (Yumoto et al. 2009), to our knowledge there is still no definite method to associate geomagnetic phenomena to earthquakes. In this report we propose to apply nonlinear and time series analyses to the MAGDAS data to extract EM precursory signals. We also would like to apply the same technique to the relation between EEJ and interplanetary magnetic field (IMF). It is well known that during magnetic storms, there is a southward reversal of the IMF. We would like to quantify its effect on EEJ.

## **2. The Equatorial Electrojet and EE-Index**

### **2.1 The Occurrence of the Equatorial Electrojet**

The equatorial electrojet or EEJ (Chapman 1951) is a narrow band of current at the E-region of the ionosphere flowing eastward along the dayside dip equator. It is caused by the enhancement of east-west Pedersen conductivity and manifests as an enhancement of the daily variations of the northward

component  $H$  of the geomagnetic field with the maximum occurring at the dip equatorial latitudes. It was first detected at Huancayo, Peru in 1922.

The existence of the equatorial electrojet can be understood by the electrodynamic of the E-region of the ionosphere. The magnetohydrodynamic generalization of Ohm's law for collisional and magnetized plasma is given by (Cravens 1997)

$$\vec{J} = \sigma_{\parallel} \vec{E}_{\parallel} + \sigma_{\perp} \vec{E}_{\perp} + \sigma_H \vec{E}_{\perp} \times \hat{b} \quad (1)$$

where  $\vec{E}_{\parallel}$  and  $\vec{E}_{\perp}$  are the components of the electric field parallel and perpendicular to the magnetic field. The first term is called parallel current density while the second term is known as Pedersen current density.  $\sigma_{\parallel}$  and  $\sigma_{\perp}$  are the corresponding conductivities. The last term is called the Hall current density and the associated conductivity is called the Hall conductivity. It is perpendicular to both the electric ( $\vec{E} = \vec{E}_{\parallel} + \vec{E}_{\perp}$ ) and magnetic ( $B\hat{b}$ ) fields and is due to the drift of the guiding centers of the charged particles, the so-called plasma drift (Bittencourt 1986).

Usually, the dipole approximation of the earth's geomagnetic field (Cravens 1997), as shown in Figure 3, is sufficient for all practical calculations. A more accurate calculation can be done by expanding the field in spherical harmonics (Jackson 1999) and by truncating the series according to the accuracy desired. This has been done by Jensen and Cain (Jensen and Cain 1962) in which they considered up to 48 terms. Using this geomagnetic field configuration, a simple model can be constructed to elucidate the existence of the equatorial electrojet (Sugiura and Cain 1966). It is well known that an eastward electric field, due to global dynamo action, drives an eastward Pedersen current (second term in Eq. (1)). If we construct a coordinate system in which the  $y$ -axis is along the north direction (along the magnetic south),  $x$ -axis along the east direction, and the  $z$ -axis along the vertical direction, then one can have

$$\vec{E} = \vec{E}_{\perp} = E_0 \hat{e}_x \quad (2)$$

and the Pedersen current can be written as,

$$\vec{J}_{\perp} = \sigma_{\perp} E_0 \hat{e}_x \quad (3)$$

At equatorial latitudes, the magnetic field can be assumed to be northward for simplicity, that is,

$$\vec{B} = B \hat{e}_y \quad (4)$$

The eastward electric field will also drive an upward Hall drift  $\vec{E}_{\perp} \times \hat{b} = E_0 \hat{e}_x \times \hat{e}_y = E_0 \hat{e}_z$ . This movement is independent of the sign of the charge and can therefore produce no net current for collisionless entity composed of equal number of electrons and positive ions. However, for collisional plasma, the electrons have higher mobility than the ions because of the latter's smaller mass. A net downward Hall current (last term in Eq. (1)) would therefore be produced. The total current density, according to Eq. (1), is therefore,

$$\vec{J} = \sigma_{\perp} E_0 \hat{e}_x - \sigma_H E_0 \hat{e}_x \times \hat{e}_y$$

$$\vec{J} = \underbrace{\sigma_{\perp} E_0}_{J_{\perp}} \hat{e}_x - \underbrace{\sigma_H E_0}_{J_H} \hat{e}_z \quad (5)$$

Considering the E-region of the ionosphere as a slab of finite thickness, inhibition of the downward Hall current results to the accumulation of electrons at the top of the slab and of positive ions at the bottom. This configuration produces a vertically upward electric field, called polarization electric field  $E_p$  that in turn produces a current of density

$$\vec{J}_p = \sigma_{\perp} E_p \hat{e}_z \quad (6)$$

The polarization electric field will acquire a steady-state value if the Hall current (second term in Eq. (5)) balances the polarization current,

$$\sigma_H E_0 - \sigma_{\perp} E_p = 0 \quad (7)$$

$$E_p = \frac{\sigma_H}{\sigma_{\perp}} E_0 \quad (8)$$

The polarization electric field will in turn drive a Hall drift

$$\vec{E}_p \times \hat{b} = \frac{\sigma_H}{\sigma_{\perp}} E_0 \hat{e}_z \times \hat{e}_y = -\frac{\sigma_H}{\sigma_{\perp}} E_0 \hat{e}_x \quad (9)$$

This drift motion will produce a current,

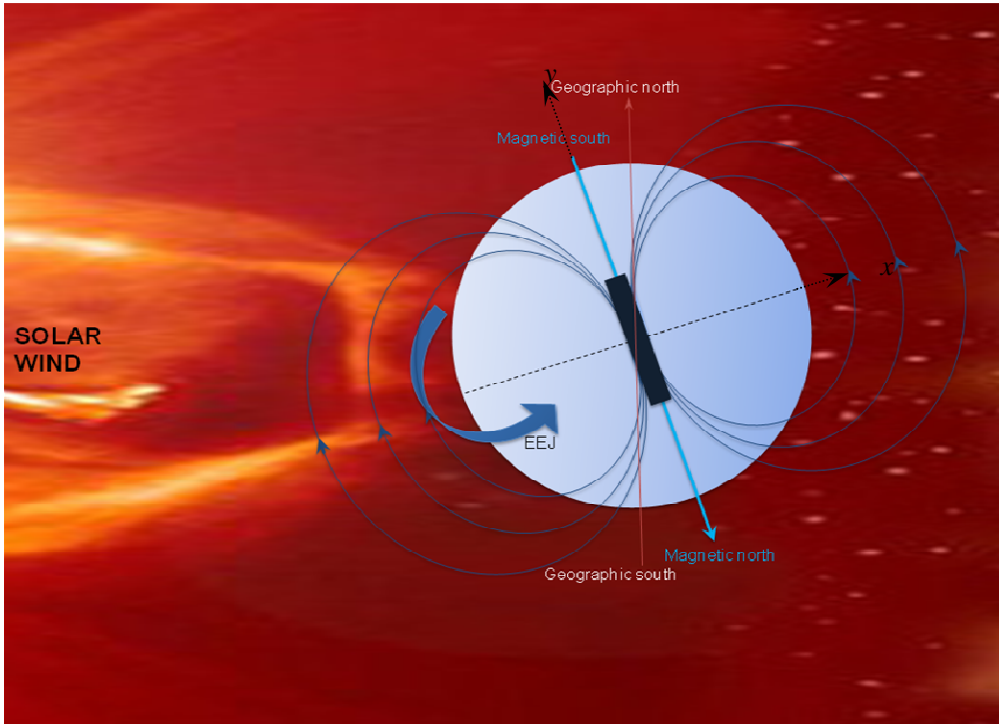


Figure 3. Schematic illustration of the dipole geomagnetic field and the equatorial electrojet (EEJ).

$$\bar{J}_p^H = \sigma_H \frac{\sigma_H}{\sigma_\perp} E_0 \hat{e}_x \quad (10)$$

The total current is therefore,

$$\bar{J}_T = \bar{J} + \bar{J}_p + \bar{J}_p^H$$

$$\bar{J}_T = \sigma_\perp E_0 \hat{e}_x + \frac{\sigma_H^2}{\sigma_\perp} E_0 \hat{e}_x = \left( \sigma_\perp + \frac{\sigma_H^2}{\sigma_\perp} \right) E_0 \hat{e}_x \quad (11)$$

which is directed eastward, the *equatorial electrojet*. The conductivity associated with EEJ is called the Cowling conductivity  $\sigma_c$  and results from the enhancement of Pedersen conductivity due to the Hall effect. It is clear from (11) that the EEJ current distribution is determined by the structure of the Cowling conductivity, which may exhibit height, latitudinal, longitudinal, day to day, and seasonal variations. This current produces an enhancement of the northward component  $H$  of the geomagnetic field at the magnetic equator. Figure 4 shows

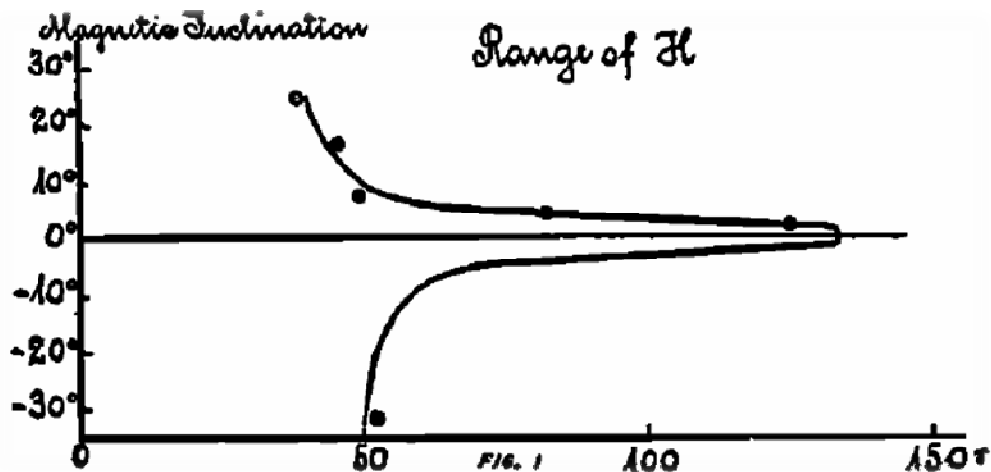


Figure 4. The variation of the northward component  $H$  of the geomagnetic field near the magnetic equator. In this figure, the locations of the observatories are expressed in terms of the magnetic inclination. The enhancement of  $H$  at the magnetic equator is the signature of the equatorial electrojet (taken from (Egedal 1947)).

The latitudinal width of the magnetic variations, which gives us an idea about the width of the EEJ, is found to be about 600 km at 75% peak value (Forbush and Cassaverde 1961, Onwumechilli 1967) with its center following the dip equator (Egedal 1947). Onwumechilli (Onwumechilli 1967) noted that the width of the EEJ varies with latitude and longitude which can be attributed to the rate of change of dip angle with latitude. For instance, it is 30% wider in Peru than in Nigeria, with dip angle change at approximately 1.9 and 2.4, respectively. Egedal (Egedal 1947) also showed that large variation of the horizontal component of the geomagnetic field occurs within 5° latitude centered on the dip equator.

To our knowledge, most ground-based geomagnetic stations used to study EEJ did not entirely cover the EEJ region. For instance, the five magnetic ground stations in Peru, which include that at Huancayo, used

by Forbush and Cassaverde (Forbush and Cassaverde 1961) did not cover the entire latitudinal EEJ band. Nevertheless, they showed that a positive excursion of the northward component  $H$  was associated with negative and positive excursions of the downward ( $Z$ ) and eastward ( $D$ ) components, respectively. Rastogi and Iyer (Rastogi and Iyer 1976) also conducted ground observations using four geomagnetic stations in India and showed the seasonal variability of EEJ driven by solar activity. These stations were all located north of the dip equator and therefore covered only half of the EEJ region.

During the French campaign in Central Africa, nine magnetic stations covering a 3000-km-long profile, from about  $4^{\circ}S$  to  $23^{\circ}N$ , restricted to a  $5^{\circ}$  longitudinal band (about  $14^{\circ} - 19^{\circ}E$ ) were deployed from November 1968 to March 1970. This relatively wide coverage enabled Fambitakoye and Mayaud (Fambitakoye and Mayaud 1976a) to devise a technique that allowed separation of the regular diurnal variation (called  $S_R$ ) of the geomagnetic field into a component characteristic of a global-scale field  $S_R^P$  ( $P$  for planetary) and an EEJ component  $S_R^E$ . This analysis technique allows investigation of several EEJ parameters in the Central African sector such as its latitudinal and temporal variations, width, location of the center (Fambitakoye and Mayaud 1976b), and discuss its day to day variability, some of its peculiar features, and the occurrence of counter electrojet or CEJ (Fambitakoye and Mayaud 1976c). Although the 1968-1970 French Central African campaign covers a relatively wide swath of the EEJ region compared to previous magnetometer arrays, it only practically covers half of this region. This has implication on the validity of the analysis adopted since the separation of  $S_R$  into  $S_R^P$  and  $S_R^E$  requires a wider latitudinal range (Onwumechilli 1967, Gupta 1973). Thus, the results of their analysis might have been biased by  $S_R^P$ .

In 1989, the International Association of Geomagnetism and Aeronomy (IAGA) initiated an international collaboration to study EEJ. Dubbed the International Equatorial Electrojet Year or IEEY (1992-1994), the collaboration involved a number of campaigns in different equatorial regions in Africa, America, and Asia. For instance, a French team deployed a number of instruments in Western Africa (Cohen 1998) consisting of a network of geomagnetic stations along the  $5^{\circ}W$  longitude extending from Lamto to Tomboucto, ionosonde, Fabry-Perot interferometer and HF radar deployed at Korhogo, and a HF sounder at Dakar. Using the geomagnetic stations spread over a distance of about 1200 km covering the entire EEJ sector, Doumouya et al. (Doumouya et al. 1998) showed the seasonal variabilities of the equatorial electrojet and counter electrojet. The northward component of the geomagnetic field  $H$  was shown to vary from dawn to dusk with maximum at local noon, a well-known signature of EEJ.  $H$  also showed diurnal and seasonal variabilities with maxima in equinoxes and minima in solstices. Other EEJ parameters such as the location of its center and half-width did not exhibit strong day-to-day and seasonal variations. The data in the Western African campaign also showed seasonal variabilities of the frequency of occurrence of the counter electrojet. It has been observed that local maxima occurred near the equinoxes and minima near the solstices.

MAGDAS's global coverage of the EEJ region provides opportunities to study the EEJ in the global scale. Although equatorial electrojet is a well studied ionospheric phenomenon, there are still many interesting and important aspects of EEJ worth investigating especially those that relate to the pressing concern of space weather. Constant monitoring of EEJ is important for studies on solar wind-magnetosphere-ionosphere-thermosphere system coupling (Yumoto and the MAGDAS Group 2006; Yumoto and the MAGDAS Group 2007) especially during the onset of magnetic storms and substorms (Kobea 1998). Energy transfer from the solar wind to the earth's space environment is mediated by the interplanetary

magnetic field (Lyon 2000). Although the earth's magnetic field is interacting with the solar wind, the flow of energy to the magnetosphere is small. However, when the field line of the IMF is connected to the field line of the earth's magnetic field at the magnetosphere, transfer of particles, momentum, and energy occurs in huge amount. It is well known that charged-particle motion is tied to the field line (Bittencourt 1986). When field lines from different regions connect, a process called *magnetic reconnection*, efficient transmission of particles from one region to another occurs. Magnetic reconnection permits two regions to be directly magnetically linked. Generally, the IMF is directed northward as shown in Figure 2A. However, during geomagnetic storms it would be directed southward allowing magnetic reconnection with the geomagnetic field at the dayside (front) as well as in the tail end as shown in Figure 2B. In this field line topology magnetospheric convection of plasma particles is enhanced allowing magnetospheric and ionospheric current systems to be enormously modified (Ondoh and Marubashi 2001).

## 2.2 The EE-Index

The focal point of this discussion is the establishment of a new index dedicated for real-time monitoring of long-term variations of EEJ using MAGDAS data (Uozumi et al. 2008). Called the *EE-Index*, this is the first step in the systematic description of EEJ in a global scale. The *EE-Index* consists of three quantities:  $ED_{St}$ ,  $EU$ , and  $EL$ . To determine  $ED_{St}$  the relative magnetic variation  $ER_S(m)$  is calculated first, where “ $S$ ” and “ $m$ ” are the MAGDAS station and universal time, respectively. This quantity is the difference between the original northward component of the magnetic field data and the median of the same component from the beginning to the end of the observation time.

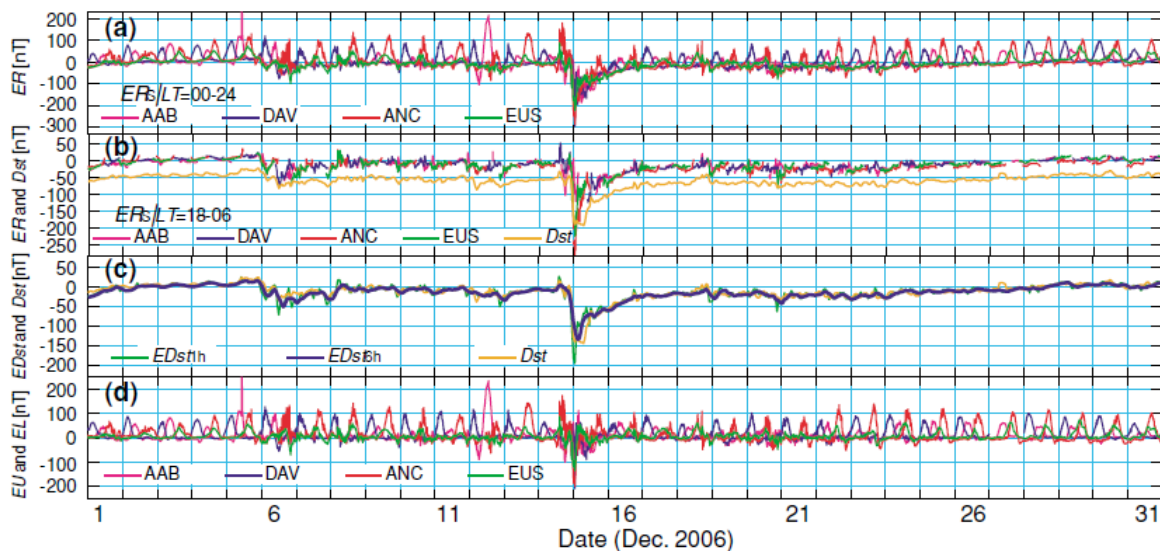


Figure 4. (a) Plot of relative magnetic variation of the  $H$ -component  $ER_S|_{LT=00-24}$  for the whole month of December 2006. (b) Nighttime relative magnetic variation  $ER_S|_{LT=18-06}$  of the  $H$  component and the real-time  $D_{ST}$ . (c)  $ED_{ST1h}$ ,  $ED_{ST6h}$ , and real-time  $D_{ST}$ . (d)  $EU$  and  $EL$  indices for EEJ and CEJ, respectively (taken from Uozumi et al. 2008).

Figure 4(a) shows the  $ER_S(m)$  for December 1-31, 2006 for the following MAGDAS stations: Addis Ababa (AAB), Davao (Dav), Ancon (ANC), and Eusebio (EUS). Figure 4(b) shows the nighttime (local time 18:00-06:00)  $ER_S(m)$  at each station for the same period. One can see that all stations have almost the same

trend of magnetic variations, which imply that nighttime  $ER_S(m)$  can be considered as common base magnetic variations. It can be seen as well that these variations follow the  $Dst$ , shown in orange in Fig. 4(b) (the  $Dst$  plot is shifted downward for clarity). The  $EDst$  (equatorial disturbance in storm time) for the 1-min data resolution is calculated using the formula:

$$EDst_{1m}(m) = \frac{\sum_{S(LT=18-06)} ER_S(m)|_{LT=18-06}}{N(m)|_{LT=18-06}} \quad (12)$$

where  $N(m)|_{LT=18-06}$  is the number of nighttime stations.  $EDst_{1m}$  is practically the average nighttime (LT=18-06) 1-min resolution  $ER_S(m)$ . In Figure 3(c) plots of  $EDst_{1h}$  (one-hour average of  $EDst_{1m}$ ),  $EDst_{6h}$  (6-hour average of  $EDst_{1m}$ ), and  $Dst$  are shown. Generally, the  $EDst$  follows the variation of the  $Dst$ . However,  $EDst_{6h}$  is closer to  $Dst$ . It is also found out that deviation of  $EDst$  from  $Dst$  decreases as more nighttime stations are included in the calculation. To extract EEJ information,  $EDst$  is subtracted from the original MAGDAS data. The result is shown in Figure 4(d). The plots that bulge out in the positive sense are signatures of EEJ while the ones in the negative sense are the so-called counter electrojet or CEJ (Gouin 1962). The former component is designated  $EU_S(m)$  and the latter  $EL_S(m)$ . These two quantities will be used to study the characteristics and variability of EEJ and CEJ, respectively. For instance it can be seen in Figure 4(d) that the troughs and dips are not synchronized with respect to station.

### 3. Seismo-Electromagnetics

#### 3.1 Electromagnetic Earthquake Precursors

In recent years, several authors have reported the observation of electromagnetic signals before, during, and after the occurrence of an earthquake in a variety of frequencies, ranging from quasi-DC to visible (Gokhberg 1982; Park et al. 1993; Oike and Yamada 1994; Hayakawa et al., 1996; Hayakawa et al. 2000; Hashimoto et al., 2002; Bleier and Freund 2005). Various mechanisms were enunciated to explain the origin of these electromagnetic signals, called earthquake precursors if they occur before the onset of an earthquake. The slow grinding of the earth's crust leading to sudden rupture accumulates stresses on the ground (Kanamori and Brodsky 2001). This process results to deformation or even breakage of crystalline rocks releasing considerable magnitude of electric current. One theory asserts that a flood of electrons and holes is released due to the breaking of atomic/molecular bonds brought about by this deformation. Indeed, rock crushing experiments showed that sundering of oxygen-oxygen bonds in minerals of fracturing rocks could produce electron-hole pairs. Electrons may manage to flow towards the mantle while holes flow towards the ground making it positively charged. Aside from electromagnetic emissions associated with these currents, charges produced may induce changes in the electrical properties of the ground such as change in conductivity (Park et al. 1993) and ionization of air in the immediate vicinity of the ground (Bleier and Freund 2005). Electric fields may be produced through the piezoelectric effect in which rock materials may develop voltages when subjected to stresses (Park et al. 1993). Magnetic fields may also be produced through piezomagnetic effect (Park et al. 1993).

Among the EM earthquake precursors, ULF anomaly is the most promising because its skin depth is comparable to the depth at which crustal activities are taking place (Yumoto et al. 2009). In the following we elucidate the possible mechanisms of ULF earthquake precursors. *Electrokinetic effect* has been pointed out by Mizutani et al. (Mizutani et al. 1976) as a possible mechanism of the generation of electric current and magnetic fields prior to the occurrence of an earthquake. Electrokinetic effect occurs when an electrolyte flows through a capillary under a pressure gradient producing electric current. A model suggesting that a porous medium can be considered as a bundle of capillaries (Scheidegger 1974) implies that an electric current is produced when a gradient in pore pressure is induced in the medium. Before an earthquake, the pore pressure at the dilatant focal region decreases while the pore pressure is the same at the surrounding region not affected by the dilatancy. Groundwater therefore flows toward the focal region inducing electric current. Byerlee (Byerlee 1995) earlier proposed that through silica deposition the gradient in pore pressure at the fault zone results to the formation of sealed compartments of various sizes and porosities. Fenoglio et al. (Fenoglio et al. 1995), basing on this model, suggested that magnetic and electric fields could be generated from nonuniform fluid flow due to the rupture of these seals. A consequence of this unsteady fluid flow is the generation of transient fields through magnetohydrodynamic and electrokinetic mechanisms. The electrokinetic signals were comparable to the ULF emissions observed before the Loma Prieta earthquake in October 1989 (Fraser-Smith et al. 1990).

Molchanov and Hayakawa (Molchanov and Hayakawa 1995) also attributed ULF electromagnetic earthquake anomalies to microfracture electrification. In this process, ULF emissions are produced by fast fluctuations of electric charges due to an ensemble of opening stress-induced microfractures or microcracks. If the rate of production of microcracks is high, the opening microcracks induce wide-band electromagnetic noise that dissipates outside the source region. This in turn produces noise-like ULF emissions on the ground surface with a cut-off frequency of about 1 Hz.

The formation of conductive region in the ground associated with earthquake may cause anomalous reflection of ULF waves from space. EM waves from space incident on the earth's surface constitute the normal magnetic-noise background. The electric field of the ULF wave from the plasmasphere induces current in the ionosphere ( $\delta \vec{J}_i = \sigma_i \delta \vec{E}$ ), which generates magnetic field  $\delta \vec{B}_i$  on the ground. The magnetic field  $\delta \vec{B}_i$  also induces a current under the ground ( $\delta \vec{J}_L$ ) which in turn produces a magnetic field  $\delta \vec{B}_L$ . The latter is the reflected magnetic field. The induced geoelectric current depends on the skin depth,

$$\delta(km) = (T/\pi\mu\sigma_L)^{1/2}$$

where  $T$  is the period of the wave,  $\mu$  is the magnetic permeability of the ground and  $\sigma_L$  is the geoconductivity. Thus the total magnetic field on the ground is  $\delta \vec{B}_G = \delta \vec{B}_i + \delta \vec{B}_L$ . The magnetic anomaly, which appears as change in polarization of the PC 3-4 magnetic pulsations, associated with earthquakes is therefore caused by the drastic change in the geoconductivity.

### 3.2 A New ULF Wave Analysis for Seismo-Electromagnetics Using MAGDAS Data

The good quality geomagnetic data obtained from MAGDAS magnetometers offer opportunity for analysis of electromagnetic anomalies associated with earthquakes. However, a clear understanding of the interaction between space environment and the lithosphere is necessary because changes in geomagnetic field are influenced more by space events rather than by lithospheric processes. A new wave analysis using MAGDAS data was introduced by Yumoto et al. (Yumoto et al. 2009) to detect these anomalies. With this new technique it is possible to identify which of the above mechanisms for ULF anomalies is at work. ULF anomalies associated with microfracturing and electrokinetics are emissions whereas the change in geoconductivity will cause change in polarization. Following Chi et al., (Chi et al., 1996), the magnitude  $A$  of the ULF wave observed on the ground is a function of the solar wind and/or magnetosphere ( $B$ ), local-time dependent ionospheric influence ( $f(LT)$ ), and lithospheric amplification factor ( $\sigma$ ) according to the equation,

$$A = Bf(LT)\sigma$$

Since space events are widespread whereas seismic activities are local, it is possible to extract precursory anomalies by comparing the amplitudes of the Pc 3-4 magnetic pulsations from a magnetic station close to the earthquake zone to a remote reference station far from the epicenter. The Yumoto analysis calls for the following steps:

- a) *calculation of the polarization ratio ( $Z/H$ ), the power ratio between the horizontal ( $H$ ) to the vertical ( $Z$ ) components of the Pc 3-4 magnetic pulsations observed at a station near the epicenter – this is conceived to capture the change in geoconductivity since its change will induce change in polarization;*
- b) *calculation of the  $H$  – and  $Z$  – power ratios ( $A_Q^H/A_{Ref}^H, A_Q^Z/A_{Ref}^Z$ ) of Pc 3,4 magnetic pulsations observed at station near the epicenter to the reference station remote from the epicenter – since seismic effect is local while geomagnetic disturbance from space is widespread, data from the remote station will eliminate the latter;*
- c) *calculation of the  $H$  – and  $Z$  – power ratios ( $A_D^H/A_Y^H, A_D^Z/A_Y^Z$ ) of each day to the one-year averaged data at a station close to the epicenter.*

This new analysis was applied to the earthquake that occurred at Kushiro (Hokkaido, Japan) on May 12, 1999 (Yumoto et al. 2009) as a case study. The  $H$ -component power ratio of Pc 3 (10 to 45-sec period) pulsation at Rikebetsu station (61 km from the epicenter) to that at Moshiri station (205 km from epicenter) is shown in Figure 5. It can be seen that the ratio increased by a factor of two a few weeks before the earthquake.

In addition, it can be observed from Figure 6 that the polarization power ratio of the vertical component to the horizontal ( $Z/H$ ) component of Pc 3 decreased about a month prior to the earthquake. In both cases there was no clear change in the Pc 4 pulsations. The power ratio of the daily values of the  $H$ - and  $Z$ -components to their yearly average at the Rikebetsu station are shown in Figure 7. It is observed that the  $H$ -component ratio for the Pc 3 pulsation increased by about three times a few weeks before the earthquake. There was no significant variation for the  $Z$ -component ratio. No precursory anomalies were

observed for the Pc 4 pulsations. However, Hattori et al. (Hattori et al. 2002) observed an apparent anomaly in the  $Z$ -component prior to the Kagoshima earthquakes in 1997.

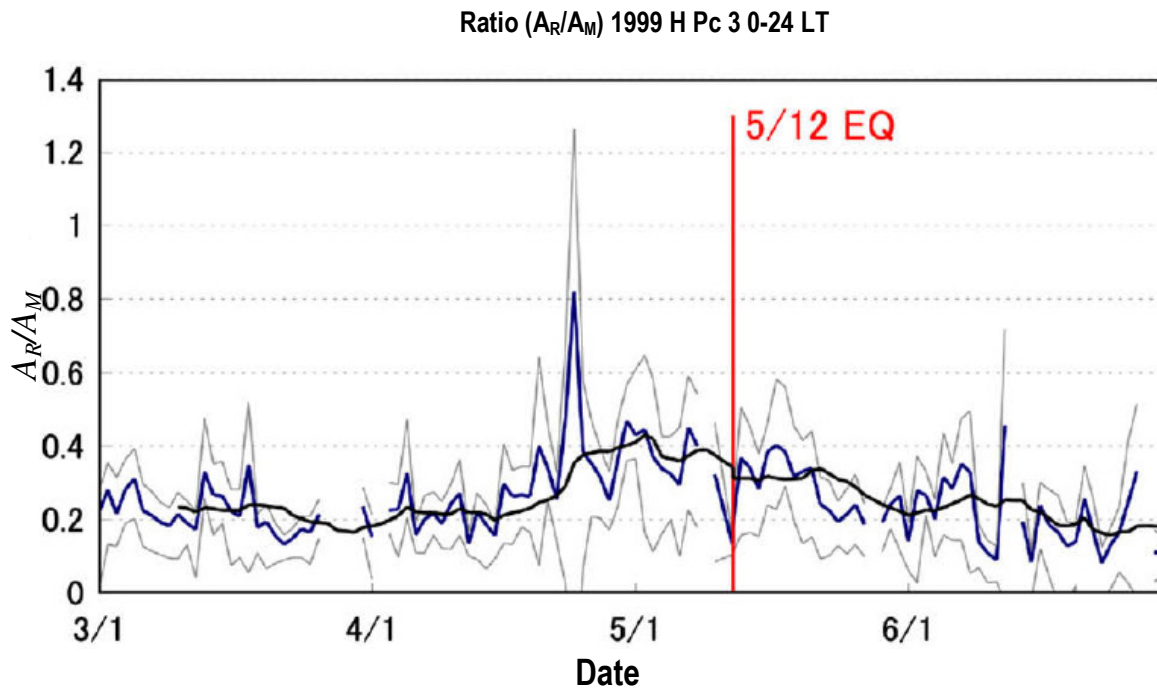


Figure 5. Plot of  $H$ -component power ratio of Pc 3 magnetic pulsation at Rikebetsu to that at Moshiri stations ( $A_R/A_M$ ). The daily values, the running average, and the standard deviation are plotted in blue, black, and gray, respectively (taken from Yumoto et al. 2009).

These observations clearly demonstrate that the search for earthquake precursors is not straightforward. Correlations of electromagnetic and seismic data are sometimes occasional and other researchers reported that there were no correlations at all. Others even refuted the existence of such correlations. In a recent paper, Campbell (Campbell 2009) refuted the existence of ULF precursor of the 1989 Loma Prieta earthquake (Fraser-Smith et al. 1990). He argued that the ULF anomaly was widespread in western United States at that time and could be attributed to a geomagnetic solar-terrestrial disturbance, in short, a geomagnetic substorm as could be seen from the  $D_{st}$  index available from the World Data Center. This is not surprising since the type of electromagnetic precursors depend on the geology of the hypocenter as exemplified by the Kushiro and Kagoshima earthquakes. This is made more complicated by the fact that mechanisms are actually poorly understood despite the fact that electromagnetic earthquake precursor was first reported more than half a century ago (Kalashnikov 1954). Thus, a robust technique to overcome these difficulties is still needed.

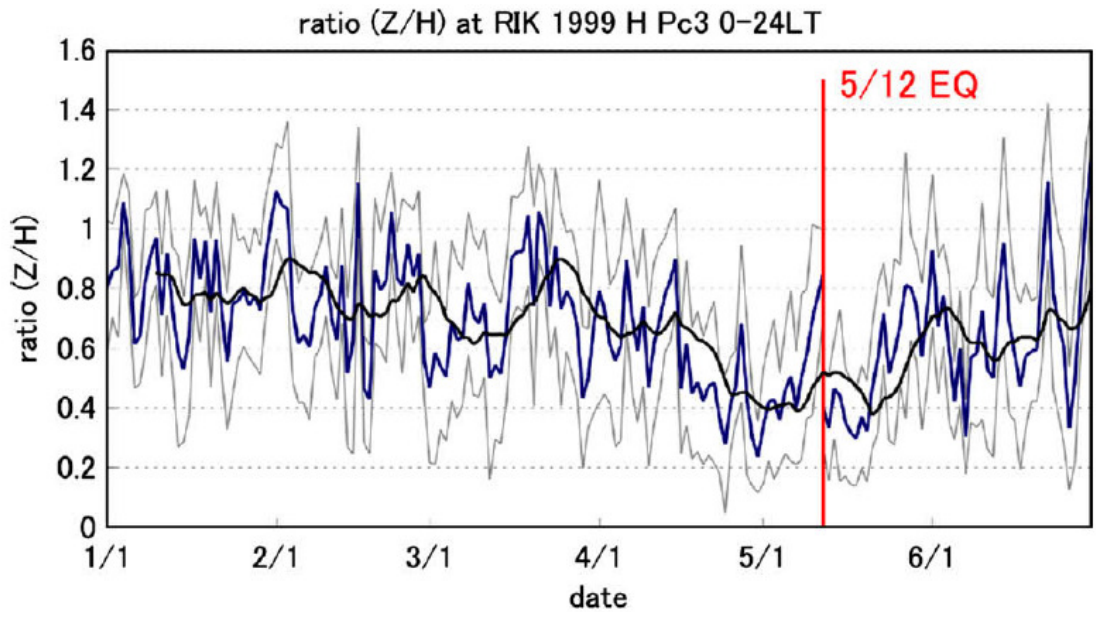


Figure 6. Pc 3 polarization ratio at the Rikebetsu station for six months. The blue curve represents the daily values, the black curve is the running average, and the gray curve is the standard deviation (taken from Yumoto et al. 2009).

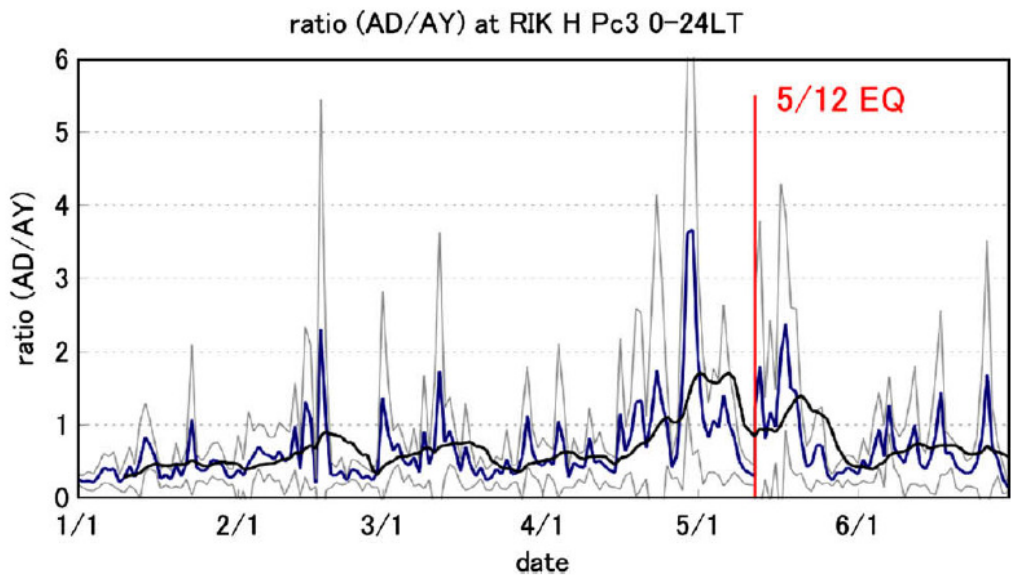


Figure 7. Plot of Pc 3 power ratio of one-day  $A_D$  (AD) to one-year average  $A_Y$  (AY), in blue, running average, in black, and standard deviation, in gray (taken from Yumoto et al. 2009).

## 4. Future Prospect: Nonlinear and Time Series Analysis of the MAGDAS Data for Studies of EEJ and Seismo-Electromagnetics

### 4.1 Investigation of the Influence of the Interplanetary Magnetic Field (IMF) on the EEJ Through Nonlinear and Time Series Analyses of the MAGDAS Data

Since the polar regions are well known entry points of energy flow from the solar wind, most studies regarding IMF were focused on its effect to the polar ionosphere (Knipp et al. 1994; Zhang et al. 2009). To our knowledge there are only a handful of studies conducted on the relationship between IMF and the equatorial electrojet. It has been reported that a northward IMF would cause a depression in the H-component of the geomagnetic field at Huancayo (Rastogi 1977; Rastogi et al. 1978). Vertical drift measurements through VHF scatter radar at the Jicamarca Radio Observatory also confirmed that a westward electric field appeared in the ionosphere. This implies that a northward IMF would cause an ionospheric westward electric field  $\vec{E} = \vec{v} \times \vec{B}_z$  associated with the solar wind velocity  $\vec{v}$  and north-south component  $\vec{B}_z$  of IMF. It is due to these facts that we would like to study the relation between the IMF and the EEJ. In this proposed study, we will quantify the relation between the IMF and the equatorial electrojet in the MAGDAS/CPMN equatorial stations located in the Philippines using nonlinear techniques during quiet times and during geomagnetic storms. The studies of Rastogi (Rastogi 1977) and Rastogi et al. (Rastogi et al. 1977) were limited at the Huancayo station. Our study will cover five geomagnetic stations (Davao, Cagayan de Oro, Cebu, Legazpi, Muntinlupa, and Tuguegarao) in the Philippines and other stations outside the Philippines within the EEJ region along the 210° magnetic meridian. However in the future, an analysis of the EEJ throughout the full longitudinal range can be done since MAGDAS, as shown in Figure 1, covers the whole dip/magnetic equator. MAGDAS also covers the polar, midlatitude, and equatorial regions in both hemispheres. A study of the equatorial electrojet using the MAGDAS/CPMN thus allows investigation of the global influences of this ionospheric current system. It is well known that the equatorial region is the terminal region of energy flows in the earth's space environment. Unlike in previous studies in which the latitudinal range of the magnetometer networks were limited, MAGDAS/CPMN's north to south ground-based magnetometer network along the 210° magnetic meridian will permit the investigation of the equatorial electrojet as part of a global current system.

Real-time magnetic data will be obtained from MAGDAS stations along the 210° magnetic meridian. IMF data will be obtained from the ACE satellite data (<http://www.srl.caltech.edu/ACE/>). We will use nonlinear measures such as fractal/multifractal structures, Hurst coefficients, algorithmic complexity and nonlinear predictability (Albano et al. 2008) to characterize and detect sudden changes in the 1-min field data, EE-index (Uozumi et al. 2008), and IMF. We will use cross-correlation coefficients, mutual information, and transfer entropy (Albano et al. 2008) to characterize correlations and information transfer between IMF and 1-min field data associated with the equatorial electrojet and EE-index. If necessary, we will develop algorithm to separate the regular diurnal variation  $S_R$  of the geomagnetic field into planetary component  $S_R^P$  and an EEJ component  $S_R^E$  (Fambitakoye and Mayaud 1976a) to elucidate the effect of the changes of the IMF on EEJ.

### 4.2 Search for Electromagnetic Earthquake Precursors in the Philippines Through Nonlinear and Time Series Analysis of the MAGDAS Data

Detection and identification of geomagnetic earthquake precursors are not easy since the geomagnetic signals are influenced more by space events. Correlations of electromagnetic and seismic data are sometimes occasional and other researchers reported that there were no correlations at all as pointed out by Campbell (Campbell 2009) regarding the 1989 Loma Prieta earthquake (Fraser-Smith et al. 1990). However, it is possible to identify EM precursors by eliminating effects arising from space events by the use of the Yumoto technique (Yumoto et al. 2009). The Yumoto technique was applied to the Koshiro earthquake in 1999 (Yumoto et al. 2009). Spectral analysis was also performed by Hattori et al. (Hattori et al. 2002) for the Kagoshima earthquakes in 1997. H-component Pc 3 anomaly was observed in Koshiro while a Z-component anomaly was observed in Kagoshima. Pc 4 anomaly was not observed. To add robustness, we will combine the Yumoto technique with nonlinear analysis (Albano et al. 2008) to the Pc 3,4 pulsations from the MAGDAS data to search for earthquake precursors in the Philippines. Earthquake information can be obtained from the United States Geological Survey (USGS) earthquake catalog. To help distinguish between space and seismic influences, we will also monitor the space environment during the time of the earthquake by using the  $D_{st}$  index available from the World Data Center for Geomagnetism at Kyoto, Japan ([http://swdc234.kugi.kyoto-u.ac.jp/dst\\_realtime/](http://swdc234.kugi.kyoto-u.ac.jp/dst_realtime/)). In particular, we will use nonlinear measures such as fractal/multifractal structures, Hurst coefficients, algorithmic complexity and nonlinear predictability to characterize and detect sudden changes in  $Z/H$ ,  $A_Q^H/A_{Ref}^H$ ,  $A_Q^Z/A_{Ref}^Z$ ,  $A_D^H/A_Y^H$ , and  $A_D^Z/A_Y^Z$ . Moreover, we will use cross-correlation coefficients, mutual information, and transfer entropy to characterize correlations and information transfer between seismic and geomagnetic data (Albano et al. 2008).

### 4.3 Workshop on Nonlinear and Time Series Analysis

To jumpstart the above research program, a workshop on nonlinear and time series analysis of the MAGDAS geomagnetic data will be held on June 23-30, 2011. This will be conducted by Dr. Alfonso Albano of Bryn Mawr College, Bryn Mawr, Pennsylvania, USA. He will come to the Philippines through the Balik-Scientist Program of the Department of Science and Technology (DOST).

### References

Akasofu, S.-I., "Polar and Magnetospheric Substorms". *Astrophysics and Space Science Library*, D. Reidel Publ. Comp., Dordrecht-Holland, 280pp, 1968.

[Albano, A., P. D. Brodfuehrer, C. J. Cellucci, X. T. Tigno, and P. E. Rapp, Time series analysis, or the quest for quantitative measures of time dependent behavior, \*Phil. Science Lett.\*, \*\*1\*\*\(1\), 18-31, 2008.](#)

Bleier, T. and F. Freund, Earthquake Alarm, *IEEE Spectrum*, **12**, 23-27, 2005.

Byerlee, J., Model for episodic flow of high pressure water in fault zones before earthquakes, *Geology*, **21**,303-306, 1993.

Bittencourt, J. A., *Fundamentals of Plasma Physics*, Pergamon Press Ltd., Oxford, England, 1986.

Boteler, D.H., R.M. Shier, T. Watanabe and R.E. Horita, "Effects of geomagnetically induced currents in the B.C. Hydro 500 kV system", *IEEE Trans. Power Delivery*, **4**, 818-823, 1989.

- Chapman, S., The equatorial electrojet as detected from the abnormal electric current distribution from Huancayo, Peru and elsewhere, *Arch. Meteorol. Geophys. Bioclimatal, Ser. A*, **368**, 1951.
- Campbell, W. H., Natural magnetic disturbance fields, not earthquake precursors, preceding the Loma Prieta earthquake, *J. Geophys. Res.*, **114**, A05307, 2009.
- Chi, P. J., C. T. Russel, G. Lee, W. J. Hughes, and H. J. Singer, "A synoptic study of Pc 3,4 waves using the Air Force Geophysics Laboratory magnetic array", *J. Geophys. Res.*, **101**(A6), 13215-13224, 1996.
- Cravens, T. E., *Physics of Solar System Plasmas*, Cambridge University Press, Cambridge, United Kingdom, 1997.
- Doumouya, V., J. Vassal, Y. Cohen, Y. Cohen, O. Fambitakoye, and M. Menvielle, Equatorial electrojet at African longitudes: first results from magnetic measurements, *Ann. Geophys.* **658**, 16, 1998.
- Egedal, J., The magnetic diurnal variation of the horizontal force near the magnetic equator, *J. Geophys. Res.*, **52**, 449, 1947.
- Fambitakoye, O. and P. N., Mayaud, The equatorial electrojet and regular daily variation  $S_R$ : I A determination of the equatorial electrojet parameters, *J. Atmos. Terr. Phys.*, **38**, 1-17, 1976a.
- Fambitakoye, O. and P. N. Mayaud, The equatorial electrojet and regular daily variation  $S_R$ : II The centre of the equatorial electrojet, *J. Atmos. Terr. Phys.*, **38**, 19-26, 1976b.
- Fambitakoye, O., and P. N. Mayaud, The equatorial electrojet and regular daily variation  $S_R$ : IV Special features in particular days, *J. Atmos. Terr. Phys.*, **38**, 123-134, 1976c.
- Fenoglio, M., M. J. S. Johnston, and J. D. Byerlee, Magnetic and electric fields associated with with changes in high pore pressure in fault zones: Application to the Loma Prieta ULF emissions, *J. Geophys. Res.*, **100**, B7, 12951-12958, 1995.
- Forbes, J. M., The equatorial electrojet, *Rev. Geophys. Space Phys*, **19**, 3, 469-504, 1981.
- Forbush, S. E. and M. Casaverde, The equatorial electrojet in Peru. In: *Pub. 620, Carnegie Inst.*, Washington, D.C., 1961.
- Fraser-Smith, A. C., A. Bernardi, P. R. McGill, M. E. Ladd, R. A. Helliwell, and O. G. Villard, Jr., Low-frequency magnetic field measurements near the epicentre of the Ms. 7.1 Loma Prieta earthquake, *Geophys. Res. Lett.*, **17**, 1465-1468, 1990.
- Gokhberg, M., Morgunov, V., and Tomizawa, I.: Experimental measurements of electromagnetic emissions possibly related to earthquake in Japan, *J. Geophys. Res.*, 1982, **87**, B9, 7824-7828.
- Gupta, J. C., On solar and lunar equatorial electrojets, *Ann. Geophys.*, **49**, 29-60, 1973.
- Hashimoto, H., Y. Enomoto, Y. Tsutsumi, and M. Kasahara, Anomalous geo-electric signals associated with recent seismic activities in Tsukuba and volcanic activity at Mt. Usu in Hokkaido, in: *Seismo-*

*Electromagnetics* (Lithosphere-Atmosphere-Ionosphere Coupling), edited by: Hayakawa, M. and Molchanov, O., Terrapub, 2002, 77-80.

Hayakawa, M., R. Kawate, O.A. Molchanov, and K. Yumoto: Results of ultra-low-frequency magnetic field measurements during the Guam earthquake of 8 August 1933, *Geophys. Res. Lett.*, 1996, **23**, 241-244.

Hayakawa M., I. Tetsuya, K. Hattori and K. Yumoto; ULF electromagnetic precursors for an earthquake at Biak, Indonesia on February 17, 1996, *Geophys. Res. Lett.* **27**(10), 1531-1534, 2000.

Hattori, K., Y. Akinaga, M. Hayakawa, K. Yumoto, T. Nagao, and S. Uyeda, ULF magnetic anomaly preceding the 1997 Kagoshima earthquakes, in *Seismo Electromagnetics: Lithosphere-Atmosphere-Ionosphere Coupling*, M. Hayakawa and O. A. Molchanov (Eds), TERRAPUB, Tokyo, pp. 19-28, 2002.

Ida, Y. and M. Hayakawa, Fractal analysis for the ULF data during the 1993 Guam earthquake to study prefracture criticality, *Nonlin. Processes Geophys.*, **13**(4), 409-412, 2006.

Jackson, J. D. Classical Electrodynamics, 3<sup>rd</sup> Ed., John Wiley and Sons, New York, 1999.

Jensen, J. C. and D. C. Cain, The interim geomagnetic field, *J. Geophys. Res.*, **67**, 3568-3569, 1962.

Kalashnikov, A. D., Potentialities of magnetospheric methods for the problem of earthquake forerunners, *Tr. Geofiz. Inst., Akad. Naul. SSSR.*, **25**, 180-182, 1954.

Kanamori, H. and E. E. Brodsky, The Physics of earthquakes, *Physics Today*, **54**, 6, 34-40, 2001.

Kobe, A. T., C. Amory-Mazaudier, J. M. Do, H. Luhr, E. Houngrinou, J. Vassal, E. Blanc, J. J. Curto, Equatorial electrojet as part of the global circuit: a case-study from the IEEY, *Ann. Geophys.*, **16**, 698-710, 1998.

Lyon, J. G., The solar wind-magnetosphere-ionosphere-coupling, *Science*, **288**(5473), 1987-1991, 2000.

Mizutani, H., T. Ishido, T. Yokokura, and S. Ohnishi, "Electrokinetic phenomena associated with earthquakes", *Geophys. Res. Lett.*, **3**(7), 365-368, 1976.

Molchanov, O. A. and M. Hayakawa, "Generation of ULF electromagnetic emissions by microfracturing", *Geophys. Res. Lett.*, **22**(22), 3091-3094, 1995.

Onwumechilli, A., "Geomagnetic variations on the equatorial zones", in *Physics of Geomagnetic Phenomena*, edited by S. Matsushita and W. H. Campbell, pp. 425-507, Academic Press, New York, 1967.

Oike, K. and Yamada, T.: "Relationship between shallow earthquakes and electromagnetic noises in the LF and VLF ranges", in: *Electromagnetic phenomena related to earthquake prediction*, (Eds) Hayakawa, M. and Fujinawa, Y., Terrapub, Tokyo, 115– 130, 1994.

Ondoh, T. and K. Marubashi, Science of Space Environment, Omsa. Ltd., Tokyo, Japan, 2001.

Otadoy, R. E. S., D. McNamara, K. Yumoto, and the MAGDAS Group, "Proposal to Use the MAGnetic Data Acquisition System (MAGDAS)/Circum-Pan Pacific Magnetometer Network (CPMN) to Study the Equatorial Electrojet: A Philippine Contribution to the International Heliophysical Year", *Earth Moon Planets*, **104**, 167-172, 2009.

Oyama, K., Y. Kakinami, J. Y. Liu, M. Kamogawa, and T. Kodama, "Reduction of electron temperature in low-latitude ionosphere at 600 km before and after large earthquakes", *J. Geophys. Res.*, 113(A117), 3367-3381, 2008.

Park, K. S., M. J. S. Johnston, T. R. Madden, F. D. Morgan, and H. F. Morrison, "Electromagnetic precursors of earthquakes in the ULF band: A review of observations and mechanisms", *Rev. Geophys.*, **31**(2), 117-132, 1993.

Rastogi, R. G., Geomagnetic Storms and electric fields in the equatorial ionosphere. *Nature*, **268**(5619), 1977.

Rastogi R. G., R. F. Woodman, and P. C. Hedgecock, "Correlated changes in the equatorial electrojet and in the interplanetary magnetic field during a geomagnetic storm", *J. Atmos. Terr. Phys.*, **40**(7), 867-869, 1978.

Rastogi, R. G and K. N. Iyer, "Quiet day variation of geomagnetic H-field at low latitudes", *J. Geomagn. Geoelectr.* **461**, 28, 1976.

Scheidegger, A. E., The physics of flow through porous media, 3<sup>rd</sup> Ed., *Univ. of Toronto Press*, pp. 126-129, 1974.

Sugiura, M., and J. C. Cain, "A Model Equatorial Electrojet", *J. Geophys. Res.*, 71(7), 1869-1877, 1966.

Uozumi, T., K. Yumoto, K. Kitamura, S. Abe, Y. Kakinami, M. Shinohara, A. Yoshikawa, H. Kawano, T. Ueno, T. Tokunaga, D. McNamara, J. K. Ishituka, S. L. G. Dutra, B. Dantie, V. Dombia, O. Obrou, A. B. Rabiou, I. A. Adimula, M. Othman, M. Fairos, R. E. S. Otadoy, and MAGDAS Group, "A new index to monitor temporal and long-term variations of the equatorial electrojet by MAGDAS/CPMN real-time data: *EE-Index*", *Earth Planets Space*, **60**, 795-790, 2008.

Yumoto, K and the CPMN Group, *Earth Planets Space* **981**, 53, 2001.

Yumoto, K. and the MAGDAS Group, "MAGDAS project and its application for space weather", ILWS Workshop 2006, Goa, February 19-24, 2006.

Yumoto, K. and the MAGDAS Group, "Space weather activities at SERC for IHY: MAGDAS", *Bull. Astr. Soc. India*, 00, 2007.

Yumoto, K., S. Ikemoto, M. G. Cardinal, M. Hayakawa, K. Hattori, J. Y. Liu, S. Saroso, M. Ruhimat, M. Husni, D. Widarto, E. Ramos, D. McNamara, R. E. S. Otadoy, G. Yumul, R. Eborra, and N. Servando, "A new ULF wave analysis for Seismo-Electromagnetics using CPMN/MAGDAS data", *Physics and Chemistry of the Earth*, **34**(6-7), 360-366, 2009.